Journal of Integrative Agriculture 2026, 25(3): 1150–1164

Available online at ScienceDirect

Journal of Integrative Agriculture



RESEARCH ARTICLE

Genome-wide characteristic and functional analyses of the *BMP* gene family reveal its role in response to directed selection in chicken (*Gallus gallus*)

Yulong Guo[1], Wanzhuo Geng[1], Botong Chen[1], Zhimin Cheng[1], Yihao Zhi[1], Yanhua Zhang[1, 2, 3], Donghua Li[1, 2, 3], Ruirui Jiang[1, 2, 3], Zhuanjian Li[1, 2, 3], Yadong Tian[1, 2, 3], Xiangtao Kang[1, 2, 3], Hong Li[1, 2, 3#], Xiaojun Liu[1, 2, 3#]

[1] *College of Animal Science and Technology, Henan Agricultural University, Zhengzhou 450046, China*
[2] *Henan Key Laboratory for Innovation and Utilization of Chicken Germplasm Resources, Zhengzhou 450046, China*
[3] *International Joint Research Laboratory for Poultry Breeding of Henan, Zhengzhou 450046, China*

Highlights

- Fourteen BMP family members were identified in chickens, evolutionarily conserved and involved in directed breeding.
- *BMP7* intronic SNPs associate with chicken growth, carcass and serum lipid traits, regulating myogenesis and adipogenesis.
- *BMP2*/*BMP6*/*GDF7* contribute to both meat- and egg-type lines, while *BMP7* favors meat-type trait development.

Abstract

The bone morphogenetic protein (BMP) gene family comprises a group of multifunctional cytokines that play important roles in limb development, bone formation, fat deposition, and reproductive traits of vertebrates. However, no systematic and comprehensive investigations of the various traits of the whole family members have been conducted, particularly in chickens. Here, we performed genome-wide screening and identified 14 *BMP* genes, which were classified into the BMP2/4, BMP5/6/7/8A, growth differentiation factor (GDF) 2/BMP10, GDF5/6/7, and GDF11/BMP3/15 subfamilies. Genetic variation pattern analysis showed that *BMP* genes were responsible for the artificial selection of commercial broilers and layers, with *BMP2*, *BMP6*, and *GDF7* likely contributing significantly to the formation of both specialized meat- and egg-type lines, whereas *BMP7* likely contributed more to the formation of meat-type lines. Genetic association analysis showed that single nucleotide polymorphisms (SNPs) in the *BMP7* intron region were associated with body weight, breast muscle weight, leg weight, abdominal fat weights and contents of total cholesterol (T-CHO), triglyceride (TG), low-density lipoprotein (LDL), and high-density lipoprotein (HDL) in serum. Additionally, gain- and loss-of-function assays demonstrated that *BMP7* promoted the proliferation, myogenic differentiation, and lipid droplet accumulation in myoblasts; enhanced lipid synthesis in hepatocytes; promoted the proliferation and inhibited adipogenic differentiation of intramuscular preadipocytes; and induced the proliferation and adipogenic differentiation of abdominal preadipocytes. These results provide novel insights into the role of *BMP* genes in chicken growth, reproductive regulation, and lipid deposition and could be used to develop genetic markers for breeding selection in chickens.

Keywords: *BMP* gene family, expression regulation, *BMP7*, myogenesis, adipogenesis

1. Introduction

Bone morphogenetic proteins (BMPs) are a class of cytokines belonging to the transforming growth factor-beta (TGF-β) superfamily. In 1965, Urist (1965) first isolated an active protein from demineralized bone matrix (DBM), and found that the protein was capable of inducing the differentiation of muscle mesenchymal cells into osteoblasts, stimulating collagen synthesis, and facilitating the formation of calcified

Received 14 December 2023; Received in revised form 15 February 2024; Accepted 28 April 2024; Available online 27 June 2024
Yulong Guo, E-mail: sxauguoyulong@126.com; #Correspondence Hong Li, E-mail: lihong19871202@163.com; Xiaojun Liu, E-mail: xjliu2008@hotmail.com

© 2026 CAAS. Publishing services by Elsevier B.V. on behalf of KeAi Communications Co. Ltd. This is an open access article under the CC BY-NC-ND license (http://creativecommons.org/licenses/by-nc-nd/4.0/). Peer review under responsibility of Editorial Board of *Journal of Integrative Agriculture*.
doi: 10.1016/j.jia.2024.06.007

bone tissue, therefore named BMP. To date, more than 30 such proteins have been identified in vertebrates, which play significant roles in skeletal muscle growth, lipid metabolism, and animal reproductive traits, alongside their involvement in ectopic osteogenesis (Shah and Rogers 2018; Ducy and Karsenty 2000; Borok *et al.* 2020).

In the BMP family, various BMP molecules exhibited structural variations due to differences in the number of amino acid residues, and possessed distinct physiological functions specific to different stages of animal growth and development (Ducy and Karsenty 2000). Based on function and amino acid sequence homology, BMP family was classified into the following 5 groups in fish: BMP2/4, BMP5/6/7/8, BMP9/10, BMP3/11/15, and BMP12/13/14 (GDF5/6/7) (Ma *et al*. 2022). Certain BMPs have been misnamed, such as BMP1, which did not belong to the BMP family because it possessed a conserved metalloproteinase domain, instead of being classified as a member of the zinc-dependent metalloprotease family (Hopkins *et al*. 2007).

The biological role of BMP1 in inducing bone and cartilage development has been extensively demonstrated (Kessler *et al.* 1996; Asharani *et al.* 2012). The BMP2/4/7 were validated as crucial growth factors involved in the embryonic development of vertebrates, regulating the proliferation of myogenic progenitors in the limbs and trunk and making a significant contribution to the formation of normal muscle tissues (Goldman *et al.* 2009; Borok *et al.* 2020). The BMP2 was involved in the regulation of bone regeneration in rabbits (Khorsand *et al.* 2017), skeletal muscle development in pigs (Hou *et al.* 2012) and adipogenic metabolism in sheep (Jin *et al.* 2022). The *BMP3* could inhibit the repair of full-thickness cartilage defects by disrupting subchondral bone through the regulation of BMP expression (Zhang *et al.* 2015). The *BMP3* was shown to be preferentially expressed in the developing ovaries of Muscovy duck and White Leghorn chicken and could promote both gonadal differentiation and follicular development (Carré *et al.* 2011; Bai *et al.* 2020). The *BMP5* was closely associated with back fat thickness in pigs (Shao *et al*. 2011). Inhibition of BMP5 expression in human adipocytes attenuated mitochondrial lipid oxidation and TG synthesis (Qiu *et al.* 2021). *In vitro* studies demonstrated that BMP6 and BMP7 could induce uncoupling protein 1 (*Ucp-1*) gene expression and lipid accumulation in primary human skeletal muscle progenitor cells (Sharma *et al.* 2014). A recent study reported that SPARC like 1 (SPARCL1) could bind to and activate BMP7, thereby activating TGF-β cellular signaling pathway to regulate the differentiation of C2C12 cells (Wang Y *et al.* 2019). The BMP8 was reported to be involved in reproductive system development, lipid metabolism and glucose homeostasis (Wang *et al*. 2014; Zhong *et al.* 2018). Moreover, germ cells and spermatogenesis in male mice were highly dependent on BMP8 (Zhao *et al.* 1998; Ying *et al.* 2000), whereas in female mice, BMP8 might promote female fertility by inducing granulosa cell proliferation *via* the Smad1/5/8 signaling pathways (Wu and Luo 2014). It was reported that the BMP9/10 group predominantly elicited the formation of bone and cartilage tissues *in vivo*, whereas BMP12/13/14 proteins specifically promoted the development of cartilage and tendon-like tissues and have almost no influence on bone-like tissue formation (Miyazono *et al.* 2010). Recent research demonstrated that BMP9 could reduce hepatic triglyceride accumulation by enhancing peroxisome proliferator activated receptor alpha (PPARα) promoter activity regulating fatty acid oxidation *via* the activation of p-Smad (Yang *et al.* 2020). The *BMP10* was located in autosomes and correlated with the body weight of Chinese Yuanbao chickens (Wang *et al.* 2016; Li *et al.* 2021). In addition to its role in axial skeleton formation, BMP11 (also called GDF11) could function as a regulator of skeletal muscle. Exogenous BMP11 protein could inhibit myoblasts differentiation in mice, humans and chicks, and induce skeletal muscle atrophy in mice (McPherron *et al.* 1999; Gamer *et al.* 2001; Jeanplong *et al.* 2012; Egerman *et al.* 2015; Zimmers *et al.* 2017). The BMP15 and GDF9 were shown to co-regulate oocyte growth and maturation, as well as granulosa proliferation and differentiation (de Castro *et al.* 2016). Although *BMP* gene family are involved in almost all biological processes during embryonic and postnatal development, to the best of our knowledge, their potential effects on reproductive traits, and the growth and development of skeletal muscle and adipose tissue in poultry have not been systematically studied.

In this study, we comprehensively analyzed the genome-wide characterization and expression profile of the chicken *BMP* gene family, as well as the contribution of their genetic variation to growth and reproductive performance. Furthermore, we characterized the expression patterns of the *BMP7* gene during myogenesis and adipogenesis and established its biological functions in hepatic lipid metabolism as well as in the cell proliferation and differentiation of myoblasts and intramuscular/abdominal preadipocytes *via* gain- or loss-of-function assays. These results provide new insights into the biological functions of the *BMP* family in chickens.

2. Materials and methods

2.1. Animals, cell preparation and culture

The experimental animals used in this study were Arbor Acres (AA) broiler purchased from a chicken breeding farm (Nanyang, China). Intramuscular fat primary preadipocytes (IMF-pre) and abdominal fat primary preadipocytes (AbF-pre) were isolated from the chicken breast muscle and abdominal adipose tissues, respectively, using an enzymatic digestion method as previously described (Zhang *et al.* 2020). Chicken myoblasts were isolated from leg muscles using the tissue block method, as previously described (Guo *et al.* 2023). Chicken hepatoma cells (LMH) were purchased from the American Type Culture Collection (ATCC, Manassas, Virginia, USA) and cultured in DMEM/F12 (BI, Haemek, Israel) supplemented with 10% fetal bovine serum (FBS, BI) supplemented with 1% penicillin/streptomycin (Solarbio, Beijing, China). The complete medium for IMF- and AbF-pre consisted of DMEM/F12 (BI) supplemented with 10% FBS (BI) and 1% penicillin/streptomycin (Solarbio). The complete medium for myoblasts consisted of high glucose DMEM (BI) supplemented with 15% FBS (BI) and 1% penicillin/streptomycin (Solarbio). All cells were cultured at 37°C with 5% CO_2.

2.2. Sequence retrieval and bioinformatics analysis of the BMP family

The *BMP* genes were identified using a hidden Markov model

(HMM) and Basic Local Alignment Search Tool (BLAST) searches (Wang Z *et al.* 2019). The amino acid sequences of the BMP family proteins from 6 species, including *Homo sapiens* (human), *Mus musculus* (mouse), *Gallus gallus* (chicken), *Pelodiscus sinensis* (turtle), *Anas platyrhynchos* (duck), and *Danio rerio* (zebrafish), were downloaded from the National Center of Biological Information (NCBI) database (https://www.ncbi.nlm.nih.gov/) (Appendix A). A phylogenetic tree was constructed using the neighbor-joining method with MEGA7.0 software, and the conserved structural domains of each BMP were identified and analyzed using the online software MEME (https://meme-suite.org/meme/index.html) and SMART (http://smart.embl.de/). We downloaded the raw data of RNA transcriptomes of the livers from pre-laying (20-wk-old) and peak-laying (30-wk-old) periods in Lushi blue-shelled egg (LS) chicken, of abdominal fat tissues from high- and low-abdominal fat percentage Gushi (GS) chickens (43-wk-old), of the ovaries from low- and high-laying rate in GS chicken (43-wk-old), of cartilage tissues from Valgus-varus deformity (VVD) and healthy Hubbard broilers, as well as of pectoral muscles from AA broiler and LS chicken at different developmental periods (embryonic d 10 [E10], E14, E18, postnatal day 1 [D1], wk 1 [W1], W3, and W5), have been uploaded to the NCBI SRA database with project accession number GSE70010 (Li *et al.* 2015), PRJNA893445, PRJNA953784, PRJNA601858 (Guo *et al.* 2020), and PRJNA729271, respectively (Appendix B). The threshold value of $|\log_2(\text{fold change})|>1$ and *P*-value≤0.05 were used to identify the differentially expressed *BMP* genes (Ji *et al.* 2020). To further verify the reliability of the sequencing data, we conducted quantitative real-time PCR (qRT-PCR) analysis of differentially expressed *BMP* genes.

2.3. Principal component analysis of genetic variations in the BMP family in multiple chicken breeds

Based on the whole-genome sequencing (WGS) of nine chicken breeds to identify SNPs in the 2,000 bp promoter, 5′-untranslated region (UTR), exons, introns, and 3'-UTR within the BMP family. The chicken breeds and their numbers used in the study are as follows: five native Chinese chicken breeds, namely GS (10 individuals), Henan Game chicken (HNG, 10 individuals), Xichuan Black Bone chicken (XCBB, 10 individuals), LS (10 individuals), and Zhengyang Sanhuang chicken (ZYSH, 10 individuals); two commercial broilers, Cobb broiler (Cobb, 30 individuals) and White Recessive Rock (WRR, 13 individuals); a commercial layer, White Leghorn (WL, 10 individuals); and an ancestral breed, Red Jungle Fowl (RJF, 5 individuals) (Appendix B). The WGS data for the nine chicken breeds were obtained from our previous studies (Wang *et al.* 2022; Guo *et al.* 2023). The *BMP* gene family responded to artificial selection, domestication from ancestors to local varieties, and selection from local varieties to commercial lines based on principal component analysis.

2.4. Association studies between SNPs within the *BMP* genes and various traits

These experiments were performed as previously described (Zhang Y *et al.* 2021; Guo *et al.* 2023). In brief, genotyping of *BMP* genes in GS hens (640 individuals) and the GS×Anka F_2 resource population (718 individuals) was performed using kompetitive allele-specific PCR (Appendices C and D). The mixed linear model was utilized to conduct an association analysis between SNP genotypes and egg production traits over different laying periods (21–25, 26–30, 31–35, 36–43, and 21–43 wk old) in GS hens, as well as 7 growth traits (0, 2, 4, 6, 8, 10, and 12-wk-old body-weight), 20 carcass traits (semi-evisceration weight, evisceration weight, semi-evisceration rate, eviscerated rate, head weight, claw weight, double pinion weight, liver weight, heart weight, gizzard weight, spleen weight, pancreas weight, breast muscle weight, leg weight, breast muscle rate, leg muscle weight, leg muscle rate, abdominal fat weight, abdominal fat rate, and Intramuscular fat content), 12 muscle fiber traits (leg muscle fiber length, leg muscle fiber width, leg muscle fiber perimeter, leg muscle fiber density, leg muscle fiber area rate, leg muscle fiber diameter, breast muscle fiber length, breast muscle fiber width, breast muscle fiber perimeter, breast muscle fiber density, breast muscle fiber area rate, and breast muscle fiber diameter), and 4 serum lipid traits (total cholesterol, triglycerides, high-density lipoproteins, and low-density lipoproteins) in the F_2 resource population.

2.5. RNA extraction, cDNA synthesis and qRT-PCR analysis

Total RNA from the collected cells or tissues was extracted using the TRIzol reagent (Vazyme Biotech, Nanjing, China) according to the manufacturer's instructions. And 1,000 ng total RNA was reverse transcribed using a HiScript Reverse Transcription Kit (Vazyme). Two-step qPCR was performed using the ChamQ Universal SYBR qPCR Master Mix (Vazyme) following the manufacturer's protocol. The gene expression levels were normalized to glyceraldehyde-3-phosphate dehydrogenase (*GAPDH*) in LMH and myoblasts, and beta-actin (*β-actin*) in IMF- and AbF-pre. qRT-PCR primers were designed using Primer-BLAST (https://www.ncbi.nlm.nih.gov/tools/primer-blast/) and were synthesized by Sunya Biotechnology Company (Zhengzhou, China) (Appendix E). The $2^{-\Delta\Delta C_T}$ method was used to calculate the relative mRNA expression (Bubner and Baldwin 2004). The qRT-PCR experiments were performed in triplicate.

2.6. Plasmid construction and siRNA oligonucleotides synthesis

The whole coding sequence (CDS) of *BMP7* was amplified by PCR and cloned into the pcDNA3.1 vector (Invitrogen, Carlsbad, CA, USA) between the *Hind*III/*Eco*RI restriction sites to construct the overexpression vector, pcDNA3.1-BMP7. Short interfering RNAs (siRNA) oligonucleotides against chicken BMP7 (si-BMP7, CUGCCGAGUUCAGGAUAUATT) and negative control (si-NC, UUCUCCGAACGUGUCACGUTT) were purchased from GenePharma Biotechnology Co., Ltd. (Shanghai, China).

2.7. Cell transfection

For myoblasts, IMF-pre, AbF-pre, and LMH cells, 1×10^5 cells

per well were seeded in a 12-well plates containing complete medium. When the cells reached 70% confluence, they were transfected with overexpression plasmids (1,000 ng per well) and siRNA oligonucleotides (50 nmol L^{-1} per well) using Lipofectamine 3000 (Invitrogen) according to the manufacturer's instructions.

2.8. Induction of adipogenic and myogenic differentiation

When IMF-pre and AbF-pre reached 90% confluence, the complete medium was replaced by adipogenic differentiation medium consisting of a final concentration of 160 μmol L^{-1} oleate (Sigma, Beijing, China). The cells were continuously induced for 48 h. LMH cells did not require adipogenic induction and were subjected to subsequent experiments 48 h after transfection. While reaching 90% confluence, myoblasts were induced for myogenic differentiation using complete medium with 2% horse serum instead of 15% FBS for 24 h, followed by a change from myogenic differentiation medium to adipogenic differentiation medium for another 24 h to detect lipid deposition. While reaching 90% confluence, myoblasts was induced for myogenic differentiation using complete medium with 2% horse serum instead of 15% FBS for 48 h to detect myogenic differentiation.

2.9. Oil Red O staining and quantification

The cells were fixed with 4% paraformaldehyde for 30 min, stained with 40% Oil Red O solution (Sigma) for 15 min, and washed 3 times with PBS. The cells were observed and photographed using an inverted fluorescence microscope (Olympus, Tokyo, Japan). To quantify cellular lipid synthesis, lipids were extracted with 100% isopropanol for 10 min, and absorbance was measured at 510 nm using a Multimode Reader (BioTek, Winooski, VT).

2.10. Measurement of intracellular triglyceride and total cholesterol

TG and T-CHO quantification kits (Applygen, Beijing, China) were used to measure the intracellular TG and T-CHO contents according to the manufacturer's instructions. Following the manufacturer's protocol, the *Omni-Easy*™ ready to use BCA Protein Quantification Kit (Yase, Shanghai, China) was used to measure total intracellular protein content to normalize the TG and T-CHO levels.

2.11. Cell proliferation assays

After 24 h of transfection with the overexpression plasmid or siRNA, the proliferation rate and viability of the cells were determined using a Cell-Light EdU Apollo 567 *In Vitro* Imaging Kit (RiboBio, Guangzhou, China) and a CCK-8 Kit (Dojindo, Kumomoto, Japan), respectively, according to the manufacturer's instructions.

2.12. Immunofluorescence analysis

After 48 h of myogenic differentiation induction, an immunofluorescence assay was performed as previously described (Li *et al.* 2019). Briefly, cells were treated with 4% paraformaldehyde for 30 min, incubated with anti-MyHC (B103; DHSB, USA; 1:50) overnight, followed by incubation with Cy3–conjugated Affinipure Goat Anti-Mouse IgG(H+L) (SA00009-1; Proteintech, USA; 1:200) for 1 h at room temperature, and finally stained with DAPI (Solarbio) for nuclear staining. Images were captured using an inverted fluorescence microscope (Olympus). The percentage of myotube area was calculated using Image ProPlus software (version 6.0; Media Cybernetics Inc., Bethesda, MD, USA).

2.13. Statistical analysis

Data are mean±SE. Differences between the 2 groups were analyzed using SPSS (version 23.0; IBM, Chicago, IL, USA) with a 2-tailed Student's *t*-test, *, $P<0.05$, and **, $P<0.01$ were considered statistically significant.

3. Results

3.1. Multi-species phylogenetic analysis

To demonstrate the phylogenetic relationship of *BMP* genes, we performed a phylogenetic analysis using BMP amino acid sequences from 6 representative species, including mammals (Human, mouse), birds (chicken, duck), reptiles (turtle), and fish (zebrafish). As shown in Fig. 1, the same members of the BMP family from different species clustered together in a single branch, indicating that they were highly evolutionarily conserved. Based on their amino acid homology, BMPs are classified into five subfamilies, namely, BMP2/4, BMP5/6/7/8, BMP3/11/15, BMP9/10, and BMP12/13/14.

3.2. Phylogenetic and gene characteristic analysis of chicken *BMP* genes

To investigate the structural characteristics of chicken *BMP* genes, we utilized the online software SMART and MEME to visualize the conserved domains and motifs of BMPs in chicken (Fig. 2). Phylogenetic analysis revealed that *BMP* genes in chickens can also be classified into five subfamilies, with the composition of the subfamily members being entirely identical to that of other species. As expected, most of the close relatives among the subfamily members had similar motif compositions. These conserved motifs varied from 15 to 40 amino acids in length (Appendix F). Analysis of the gene structure showed that BMP1 protein with a typical ZnMc structural domain does not belong to the *BMP* gene family, while each member of BMP family contains a typical TGF-β domain, and four identified motifs (motif 1/2/3/4) can be mapped to the TGF-β domain (Appendix G), which are related to myogenesis or adipogenesis.

3.3. Genetic variation patterns of *BMP* genes in response to directed breeding in chickens

To investigate the contribution of *BMP* genes to natural and artificial domestication from ancestral red jungle fowl to local strains, as well as the directed breeding from local breeds to commercial strains, we conducted screening and statistical analysis of SNPs in the promoter region, 5′ UTR, coding exons, introns, and 3′ UTR, of the 14 members of the *BMP* gene family. A total of 5,539 SNPs were screened and used to assess the population structure using the principal component analysis (PCA) clustering technique. PCA revealed strong genetic differentiation among the

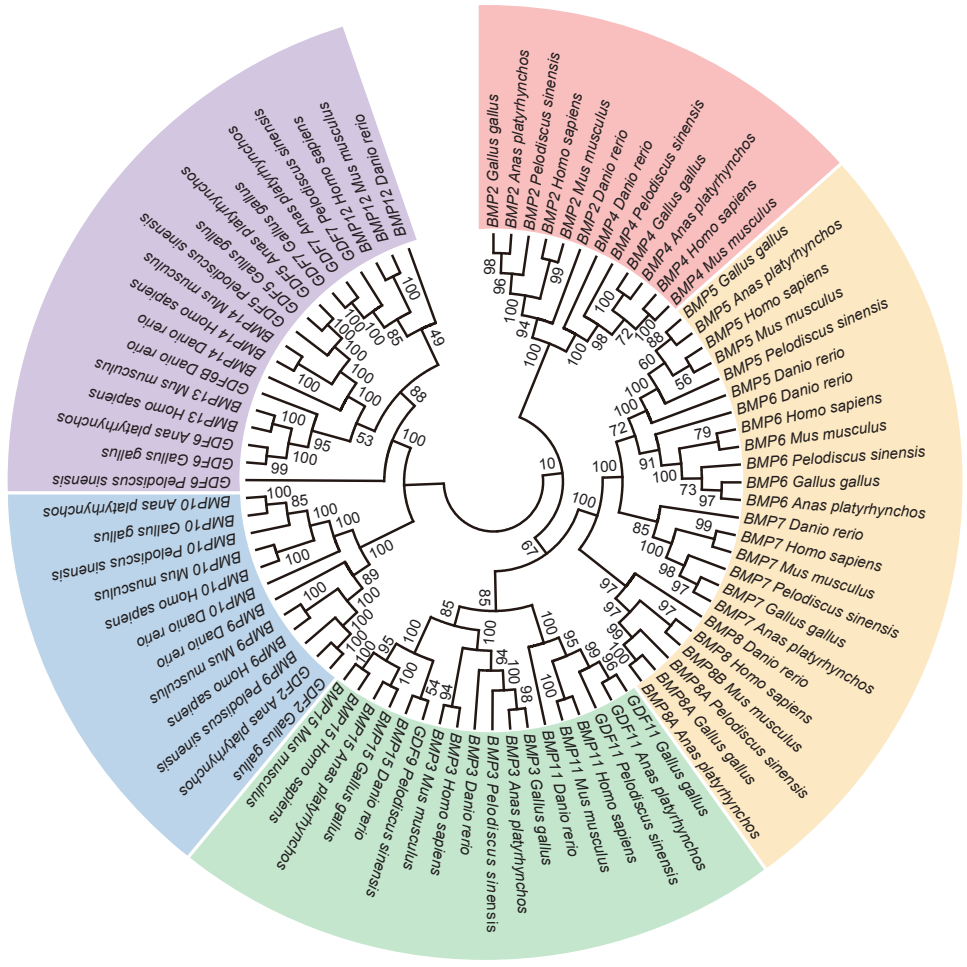


Fig. 1 Phylogenetic analysis of the amino acid sequences of *BMP* genes among species, including human (*Homo sapiens*), mouse (*Mus musculus*), chicken (*Gallus gallus*), duck (*Anas platyrhynchos*), turtle (*Pelodiscus sinensis*), and zebrafish (*Danio rerio*).

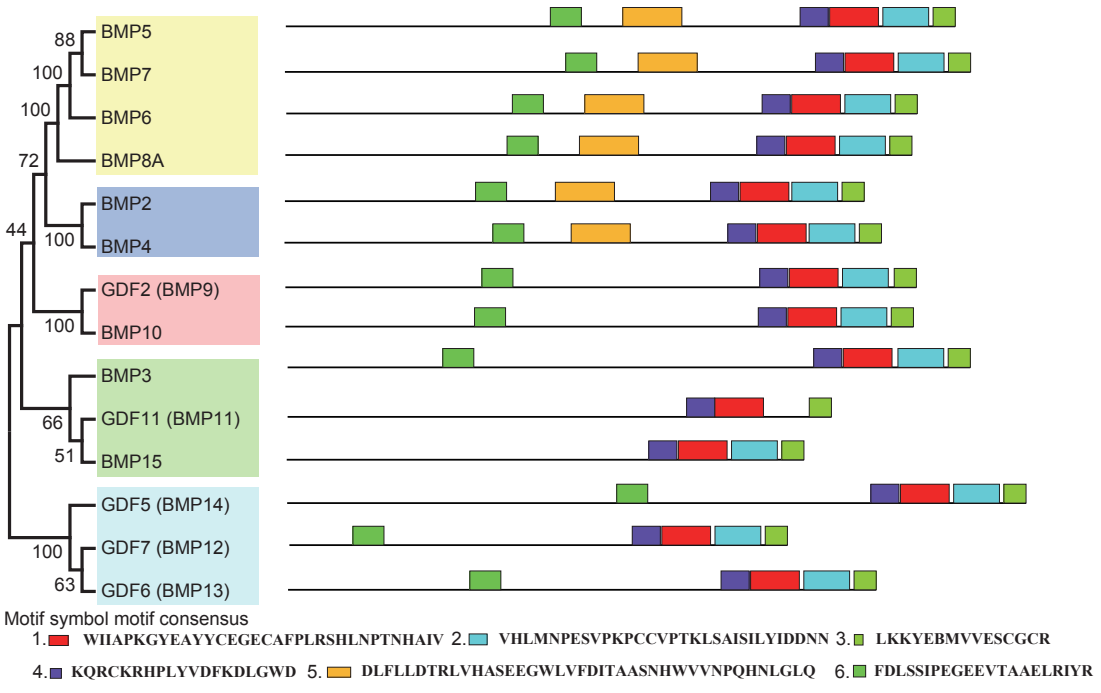


Fig. 2 Phylogenetic and motif analyses of the chicken BMP family. For the purpose of clarity, the parenthetical gene names represent the nomenclature used for the corresponding genes in other species, which are not applicable to chicken.

local breeds and commercial strains (Fig. 3-A). Based on the PC1 axis, WL and WRR exhibited clear separation and were partially separated from Cobb, suggesting that *BMP* genes contribute to growth, development, and egg-laying performance in chickens. Furthermore, PCA based on SNPs identified in multiple regions of each member within the *BMP* gene family showed that individual genes within the *BMP* gene family exhibited various degrees of contribution to the specialization of commercial strains (Fig. 3-B–O). The results showed that during the directed breeding process of chicken, *BMP2*, *BMP6*, and *GDF7* played a prominent role in the formation of both specialized meat- and egg-type lines, whereas *BMP3* and *GDF5* likely contributed more than other genes to the formation of the egg-type line (Fig. 3-B, F, and L). Additionally, *BMP7* was found to contribute more to the specialization of commercial strains than did the other genes, specifically in the formation of the meat-type line (Fig. 3-G).

3.4. Associations between SNP genotypes of the *BMP* genes and traits of egg-laying performance, growth, carcass, and serum lipid levels

Based on the above PCA results, genetic variations in *BMP* genes arise from the artificial selection of commercial broilers and laying hens. To further validate the potential impact of *BMP* genes on egg-laying performance, we genotyped the SNPs of *BMP* genes in 640 GS hens and analyzed the correlation between the SNPs and egg-laying traits. The results indicated that the SNPs located in the promoter regions of these genes were significantly correlated with the egg-laying traits (Appendix C). For example, SNPs in the *BMP2* (3_15207474), *BMP3* (4_45455884, 4_45456016, 4_45456042, and 4_45455884), *GDF7* (3_101915948, 3_101916138, and 3_101916281), *GDF5* (20_1253426, 20_1254031, 20_1254383, and 20_1254422) promoter region, and *BMP6* exon region (2_64399745) were associated with egg number of 26–30 wk and the total egg number. Moreover, correlation analysis between SNP genotypes of *BMP* genes and growth, carcass, and serum lipid traits in 718 individuals at 12-wk-old in F_2 resource population showed that SNP 2_64439464 in the *BMP6* intron region was associated with body weight, breast muscle weight, and leg muscle weight, and abdominal fat weight, and the SNPs 20_11688500 and 20_11688970 in the *BMP7* intron region were associated with the 0/2-wk-old body weight, breast muscle weight, leg weight, abdominal fat weight, T-CHO, TG, LDL, and HDL (P<0.05; Appendix D).

3.5. Multi-tissue transcriptome analysis

To investigate the potential functions of *BMP* genes, we integrated transcriptomic data from multiple tissues

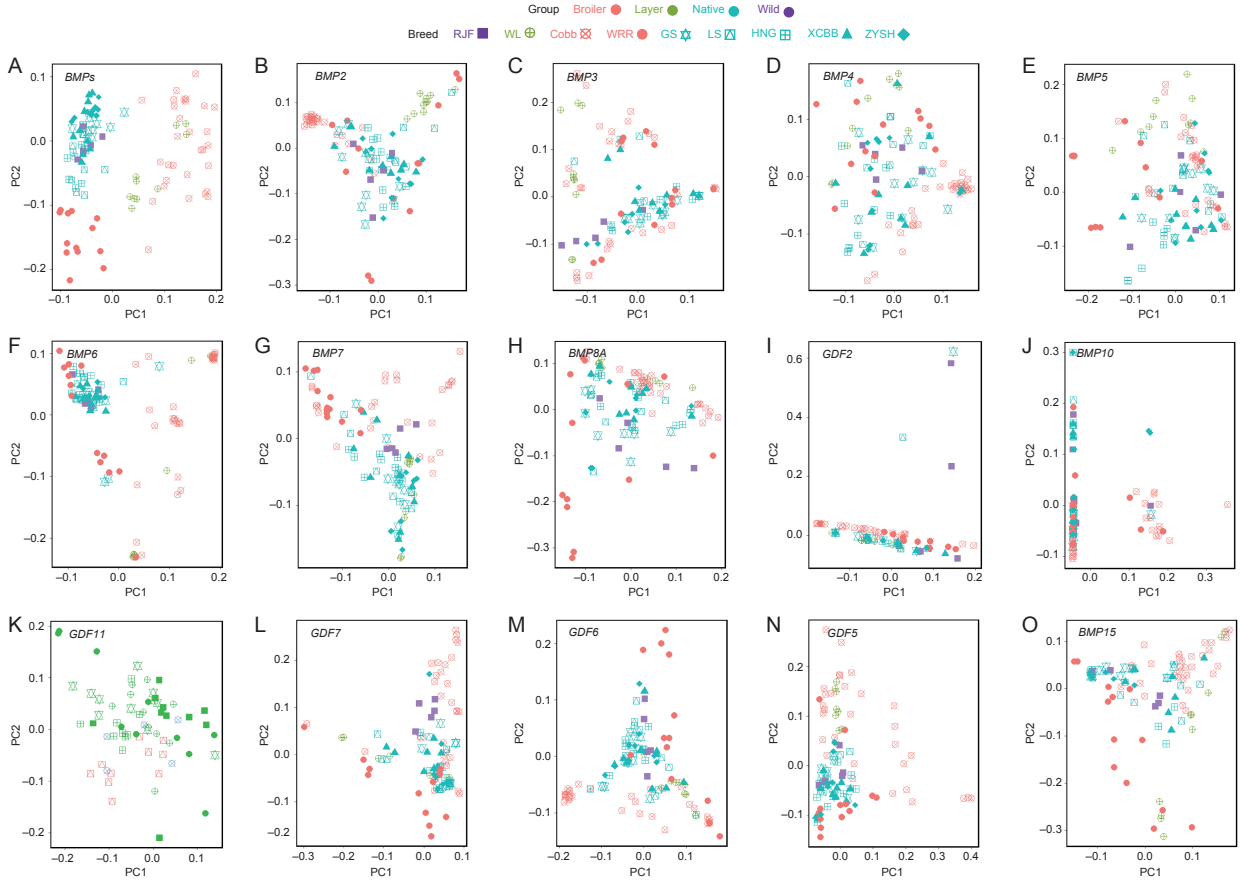


Fig. 3 Principal component analysis. A–O, the plots were established according to the SNPs mapped to (A) the whole-genome in *BMP* genes, (B) *BMP2*, (C) *BMP3*, (D) *BMP4*, (E) *BMP5*, (F) *BMP6*, (G) *BMP7*, (H) *BMP8A*, (I) *GDF2*, (J) *BMP10*, (K) *GDF11*, (L) *GDF7*, (M) *GDF6*, (N) *GDF5*, (O) *BMP15*.

under various physiological conditions and identified the differentially expressed *BMP* genes. The Venn diagram revealed differentially expressed *BMP* genes in the abdominal fat, liver, cartilage, ovaries, and pectoral muscle tissues. The qRT-PCR results validated the reliability of the transcriptomic data (Fig. 4; Appendix H). Further analysis showed that the expression level of the *BMP7* gene was significantly higher in the abdominal fat tissue of GS with a high-abdominal fat percentage and in the liver tissue of 30-wk-old LS chickens, whereas it was significantly lower in the pectoral muscle tissue of 1-wk-old AA broilers than that in LS chickens (P<0.05; Fig. 4-A, B and E). Furthermore, *BMP2-6* and *GDF11* were differentially expressed in the transcriptomic datasets (Fig. 4-A–F).

3.6. Tissue expression profile of *BMP7* gene and its expression pattern during myogenesis and adipogenesis

We used qRT-PCR to detect the expression of *BMP7* in multiple tissues of 3-wk-old AA broiler chickens and found that *BMP7* was widely expressed in different tissues, with relatively higher expression levels in the liver and abdominal fat tissues (Fig. 5-A). We constructed induction differentiation models of myoblasts, IMF-pre, and AbF-pre to investigate the expression characteristics of *BMP7* during proliferation and differentiation of myoblasts, IMF-pre, and AbF-pre. The results showed that as differentiation progressed, myoblast-myotube fusion, and adipocyte-lipid deposition gradually increased, indicating that the cell model was successfully constructed (Fig. 5-B, D, and F). qRT-PCR analysis showed that the expression of *BMP7* in myotubes gradually increased during the proliferation and differentiation stages (Fig. 5-C). *BMP7* expression levels significantly decreased during the proliferation and differentiation stages of IMF-pre, whereas it significantly increased during the proliferation and early differentiation phase (DM1-2) of AbF-pre, followed by a continuous decrease (DM3, 5, 7, and 9) (Fig. 5-E and G). Overall, our results suggested that *BMP7* plays different roles during the proliferation and differentiation stages of myoblasts, IMF-pre, and AbF-pre.

3.7. The *BMP7* regulates hepatic lipid synthesis

To elucidate the function of *BMP7* in LMH cells, we performed gain- and loss-of-function assays to evaluate its effects on hepatocyte lipid metabolism. qRT-PCR results showed that *BMP7* was successfully overexpressed in LMH cells, with approximately 3,390-fold increase in *BMP7* gene expression (P<0.01; Fig. 6-A). Overexpression of *BMP7* significantly increased intracellular lipid droplets and TG and T-CHO contents in LMH cells (P<0.01; Fig. 6-B–D). Accordingly,

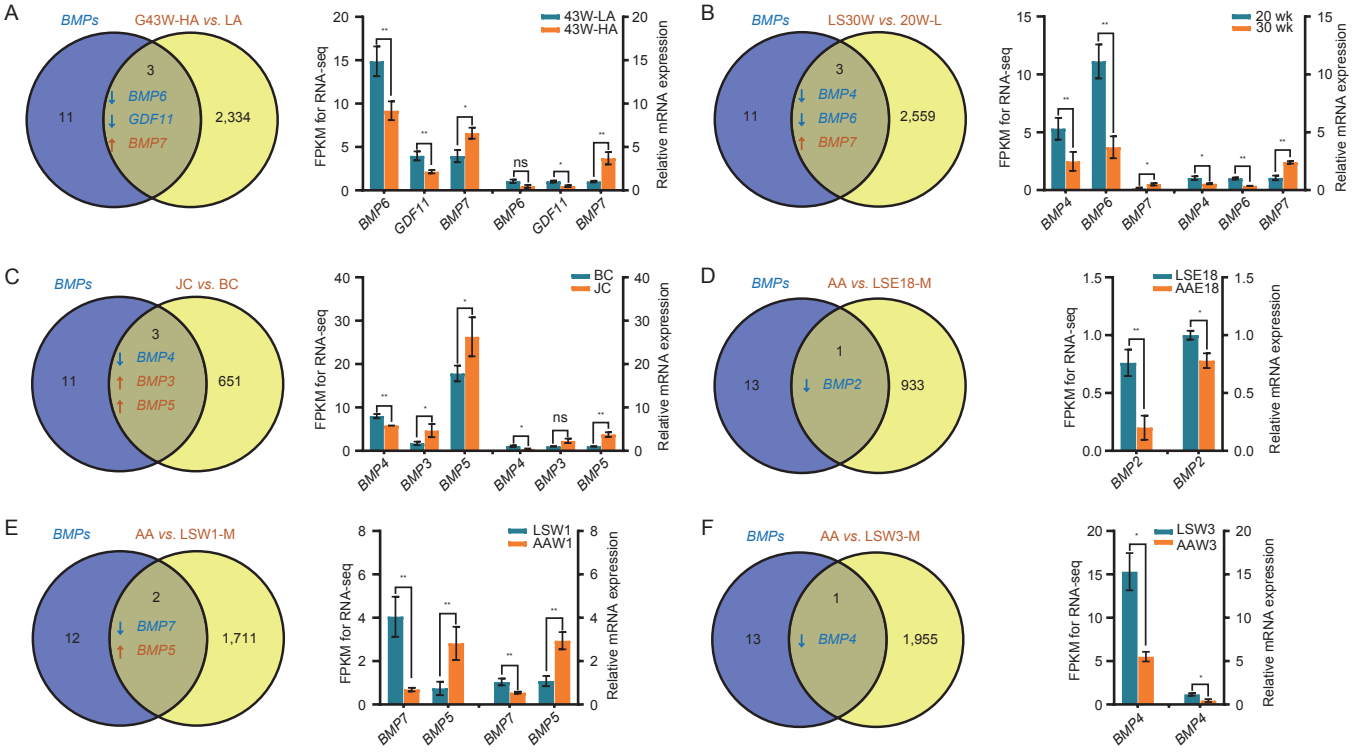


Fig. 4 Multitissue transcriptome analysis and qRT-PCR validation of differentially expressed *BMP* genes. A, Venn diagram of differentially expressed *BMP* genes and qRT-PCR validation in HA and LA groups. HA and LA represent high- and low-abdominal fat rate Gushi (GS) abdominal fat tissue. B, Venn diagram of the differentially expressed *BMP* genes and qRT-PCR validation in the LS liver tissues at 20 and 30 wk. L, liver. C, Venn diagram of the differentially expressed *BMP* genes and qRT-PCR validation in the BJ and BC groups. JC represents healthy chicken cartilage tissue and BC represents the Valgus-varus deformity of the chicken cartilage tissue. D–F, Venn diagram of differentially expressed *BMP* genes and qRT-PCR validation in Arbor Acres (AA) broilers and Lushi blue-shelled egg (LS) pectoral muscles at E18 (D), W1 (E), and W3 (F). M, pectoral muscle. Data are mean±SE (n≥3). *, P<0.05; **, P<0.01; ns, not significant.

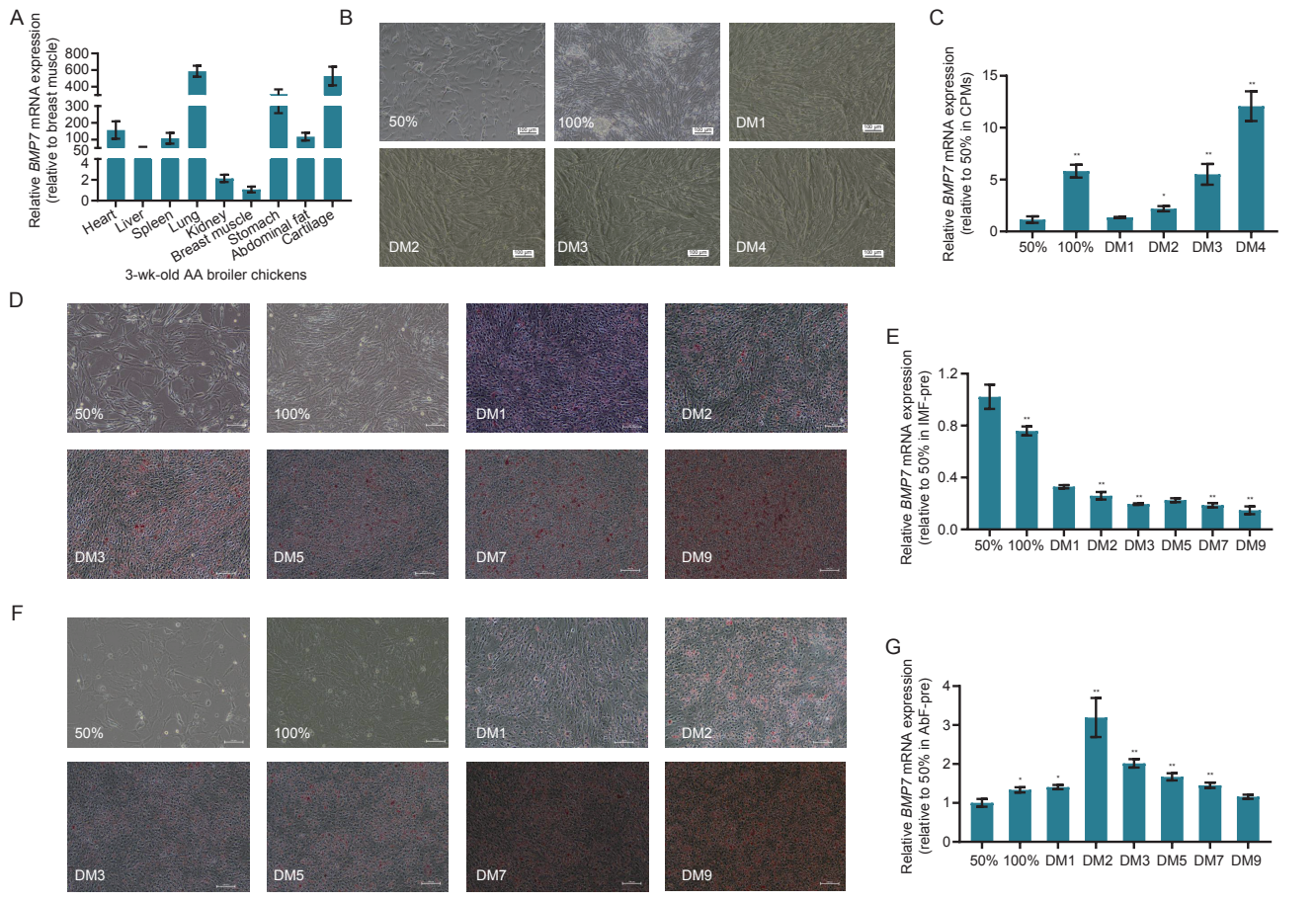


Fig. 5 Analysis of *BMP7* expression characteristics. A, Arbor Acres (AA) broiler tissue expression profile of *BMP7*. B, D, and F, cell culture images of myoblasts (B), intramuscular fat primary preadipocytes (IMF-pre) (D), and abdominal fat primary preadipocytes (AbF-pre) (F) during proliferation and differentiation. Proliferation periods, 50 and 100% confluency; differentiation periods, DM1–4 (myoblasts), DM1–3, 5, 7, and 9 (IMF- and AbF-pre); DM, differentiation day; Oil Red O staining of IMF- and AbF-pre during various differentiation stages. C, E, and G, relative *BMP7* expressions during myoblasts (C), IMF-pre (E), and AbF-pre (G) proliferation and differentiation. Data are mean±SE(n≥3). *, P<0.05; **, P<0.01; ns, not significant.

genes related to TG biosynthesis, including fatty acid synthase (*FASN*) and ATP citrate lyase (*ACLY*); genes related to TC biosynthesis, including 3-hydroxy-3-methylglutaryl-CoA reductase (*HMGCR*); and genes related to lipid transport, including apolipoprotein B (*APOB*) and apovitellenin 1 (*APOV1*), were significantly activated upon *BMP7* stimulation (P<0.05; Fig. 6-E). Conversely, *BMP7* expression was significantly reduced by approximately 76.14% in the si-BMP7 group compared to that in the si-NC group (P<0.01; Fig. 6-F). The *BMP7* knockdown significantly decreased intracellular lipid droplets, TG, and T-CHO contents in LMH cells (P<0.05; Fig. 6-G–I). Following *BMP7* knockdown, the relative mRNA expression levels of the abovementioned lipid-related genes, including *FASN*, *ACLY*, *HMGCR*, *APOB*, and *APOV1* were significantly decreased (P<0.05; Fig. 6-J). Collectively, these results indicated that *BMP7* promotes hepatic lipid synthesis.

3.8. The *BMP7* regulates the proliferation, differentiation, and lipid synthesis of myoblasts

To elucidate the function of *BMP7* in myoblasts, we evaluated its effects on cell proliferation, differentiation, and lipid synthesis in myoblasts *via* gain- and loss-of-function assays by transfecting pcDNA3.1-BMP7 and si-BMP7, respectively. Compared to corresponding control group, the *BMP7* mRNA expression level exhibited an approximately 26-fold increase in myoblasts transfected with *BMP7* gene overexpression vector, and an approximately 48.04% decrease in myoblasts transfected with *BMP7* gene siRNA oligonucleotides (Fig. 7-A). The *BMP7* overexpression significantly increased the viability of myoblasts, whereas the opposite effect was observed upon *BMP7* knockdown, as evidenced by the CCK-8 assay (P<0.01; Fig. 7-B). In addition, the upregulation of *BMP7* expression led to a decrease in the proportion of cells in the G0/G1 phase and a significant increase in the proportion of cells in the S phase. Conversely, *BMP7* knockdown resulted in a significantly lower percentage of myoblasts in the S phase (P<0.05; Fig. 7-C; Appendix I). Accordingly, upon *BMP7* stimulation, pro-proliferative genes, including cyclin-dependent kinase 1 (*CDK1*), cyclin D1 (*CCND1*), cyclin B2 (*CCNB2*), and proliferating cell nuclear antigen (*PCNA*), were significantly activated, and anti-proliferative genes, including cyclin-dependent kinase inhibitor 1A (*CDKN1A*) and cyclin-dependent kinase inhibitor 2 B (*CDKN2B*), were significantly suppressed. Moreover, *BMP7*

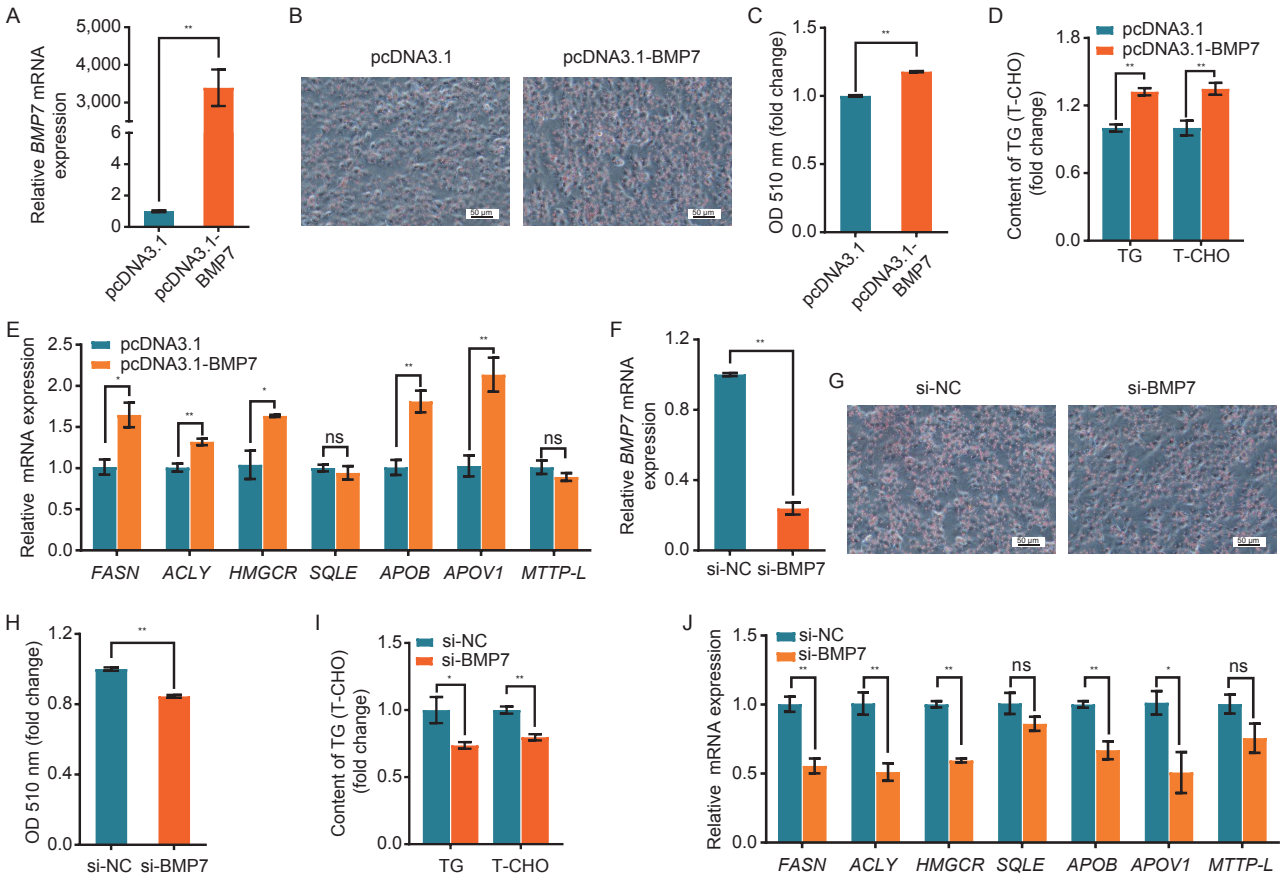


Fig. 6 *BMP7* promotes hepatic lipid synthesis. A, *BMP7* mRNA relative expression in chicken hepatoma cells (LMH) cells after transfection with pcDNA3.1 or pcDNA3.1-BMP7. B, Oil Red O staining analysis of the lipid droplet content in pcDNA3.1 or pcDNA3.1-BMP7-overexpressing LMH cells. C, after 48 h of transfection of LMH cells with pcDNA3.1 or pcDNA3.1-BMP7, Oil Red O was extracted with 100% isopropanol and the optical density of the solution was measured at 510 nm. D, quantification of TG and T-CHO contents in pcDNA3.1 or pcDNA3.1-BMP7 overexpression LMH cells. E, mRNA expression levels of *FASN*, *ACLY*, *HMGCR*, *SQLE*, *APOB*, *APOV1*, and *MTTP-L* in LMH cells after transfection with pcDNA3.1 or pcDNA3.1-BMP7. F, *BMP7* mRNA relative expression in the LMH transfected with si-NC or si-BMP7. G, Oil Red O staining analysis of the lipid droplet content in si-NC or si-BMP7 knockdown LMH cells. H, after 48 h of transfection of LMH cells with si-NC or si-BMP7, Oil Red O was extracted with 100% isopropanol and the optical density of the solution was measured at 510 nm. I, quantification of TG and T-CHO contents in si-NC or si-BMP7-overexpressing LMH cells. J, the mRNA expression levels of *FASN*, *ACLY*, *HMGCR*, *SQLE*, *APOB*, *APOV1*, and *MTTP-L* in LMH transfected with si-NC or si-BMP7. Data are mean±SE (n≥4). *, P<0.05; **, P<0.01; ns, not significant.

knockdown had an opposite effect (P<0.05; Fig. 7-D). After myogenic differentiation for 48 h, myosin heavy chain (MyHC) immunofluorescence staining and qRT-PCR results showed that *BMP7* overexpression significantly increased the area and percentage of myotubes as well as the relative mRNA expression of myogenic differentiation 1 (*MyoD*), myogenin (*MyoG*), *MyHC*, and myoblasts fusion factor (*Myomaker*) (myoblast differentiation marker genes), whereas the opposite effect was observed upon *BMP7* knockdown (Fig. 7-E–H). After adipogenic differentiation for 24 h, the overexpression of *BMP7* significantly increased intracellular lipid droplets and TG content in myoblasts, whereas *BMP7* knockdown inhibited cellular lipid deposition. (P<0.05; Fig. 7-I–L). The lipogenesis-related genes, including peroxisome proliferator activated receptor gamma (*PPARγ*), CCAAT/enhancer-binding protein alpha (*C/EBPα*), *FASN*, lipoprotein lipase (*LPL*), fatty acid binding protein 4 (*FABP4*), and fatty acid binding protein 5 (*FABP5*), were significantly activated upon *BMP7* stimulation. Conversely, *BMP7* knockdown had an opposite effects on these genes (P<0.05; Fig. 7-M). Taken together, these results indicate that *BMP7* has a positive regulatory effect on cell proliferation, differentiation, and lipid synthesis in chicken myoblasts.

3.9. The *BMP7* regulates proliferation and adipogenic differentiation of IMF-pre

To elucidate the function of *BMP7* in IMF-pre, we transfected the plasmid (pcDNA3.1 and pcDNA3.1-BMP7) and small interfering RNA (si-NC and si-BMP7) into IMF-pre to evaluate their effects on cell proliferation and adipogenic differentiation. Compared to corresponding control group, the *BMP7* mRNA expression level exhibited an approximately 2,645-fold increase in myoblasts transfected with *BMP7* gene overexpression vector, and an approximately 70.63% decrease in myoblasts transfected with *BMP7* gene siRNA oligonucleotides (Fig. 8-A). As

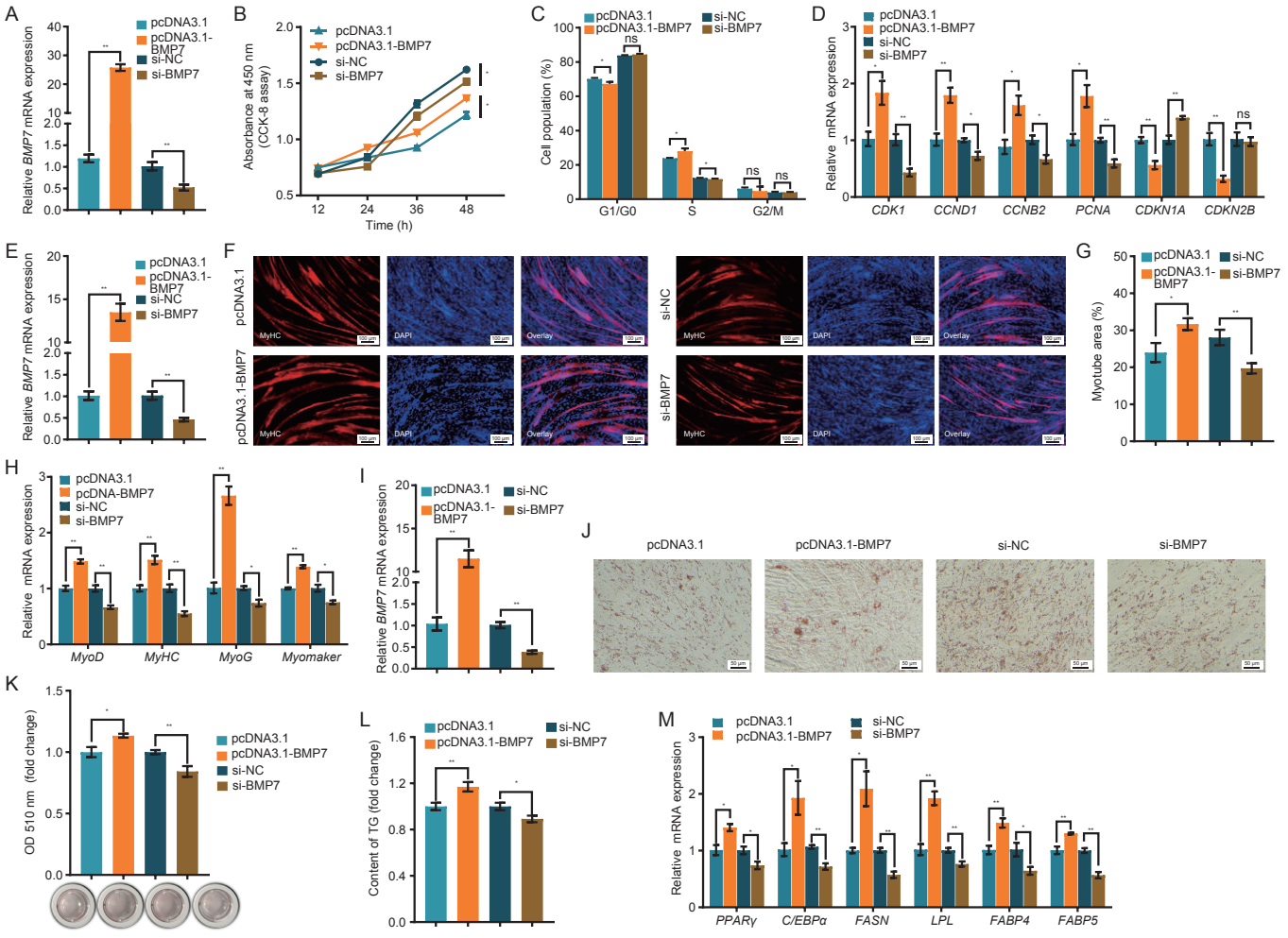


Fig. 7 *BMP7* promotes myoblasts proliferation and differentiation, and induces lipid synthesis. A, *BMP7* relative expression in myoblasts was assessed 24 h after transfection with the listed nucleic acids. B, cell viability was determined using the CCK-8 assay. C, experimental and statistical results of cell cycle analysis by flow cytometry. D, relative expression of *CDK1*, *CCND1*, *CCNB2*, *PCNA*, *CDKN1A*, and *CDKN2B*. E, *BMP7* relative expression in myoblasts 48 h after transfection with the listed nucleic acids and induction of myoblasts differentiation. F, MyHC immunofluorescent staining of myoblasts. Scale bar=100 μm. G, myotube area (%) of myoblasts. H, relative expression levels of *MyoD*, *MyHC*, *MyoG*, and *Myomaker*. I, *BMP7* relative expression in myoblasts 48 h after transfection with the listed nucleic acids and the induction of adipogenic differentiation. J, Oil Red O staining of adipogenically differentiated chicken myoblasts. Scale bar=50 μm. K, spectrophotometric analysis of lipid droplet content by Oil Red O staining of adipogenically differentiated chicken myoblasts. L, quantification of the intracellular TG content. M, the relative expression of *PPARγ*, *C/EBPα*, *FASN*, *LPL*, *FABP4*, and *FABP5*. Data are mean±SE(n≥3). *, P<0.05; **, P<0.01; ns, not significant.

determined by EdU assays, *BMP7* overexpression significantly increased cell proliferation in IMF-pre, whereas the opposite effect was observed from *BMP7* knockdown (P<0.01; Fig. 8-B and C). The *BMP7* overexpression also significantly increased cell viability, whereas *BMP7* knockdown had the opposite effect (P<0.05; Fig. 8-D). Moreover, the upregulation of *BMP7* expression resulted in a decrease in the proportion of cells in the G0/G1 phase and a significant increase in the proportion of cells in the S phase (P<0.05). Conversely, *BMP7* knockdown resulted in a notable arrest of the cell cycle in the G1/G0 phase and a significant reduction in the S phase in IMF-pre (P<0.01; Fig. 8-E; Appendix J). Additionally, *BMP7* overexpression resulted in significantly upregulated expression levels of *CDK1*, *CCND1*, *CCNB2*, and *PCNA* and downregulated expression levels of *CDKN2B*, whereas *BMP7* knockdown had the opposite effect (P<0.05; Fig. 8-F). After adipogenic differentiation for 48 h, the overexpression of *BMP7* significantly inhibited intracellular lipid droplets and TG contents in IMF-pre, whereas *BMP7* knockdown increased intracellular lipid deposition (P<0.01; Fig. 8-G–J). The lipogenesis-related genes, including *PPARγ*, *C/EBPα*, *LPL*, *FABP4*, and *FABP5*, were significantly repressed upon *BMP7* stimulation, whereas *BMP7* knockdown presented opposite effects (P<0.05; Fig. 8-K). Collectively, these data demonstrated that *BMP7* promotes IMF-pre proliferation and inhibits adipogenic differentiation.

3.10. The *BMP7* regulates proliferation and adipogenic differentiation of AbF-pre

To elucidate the function of *BMP7* in AbF-pre, we transfected the plasmids (pcDNA3.1 and pcDNA3.1-BMP7) and

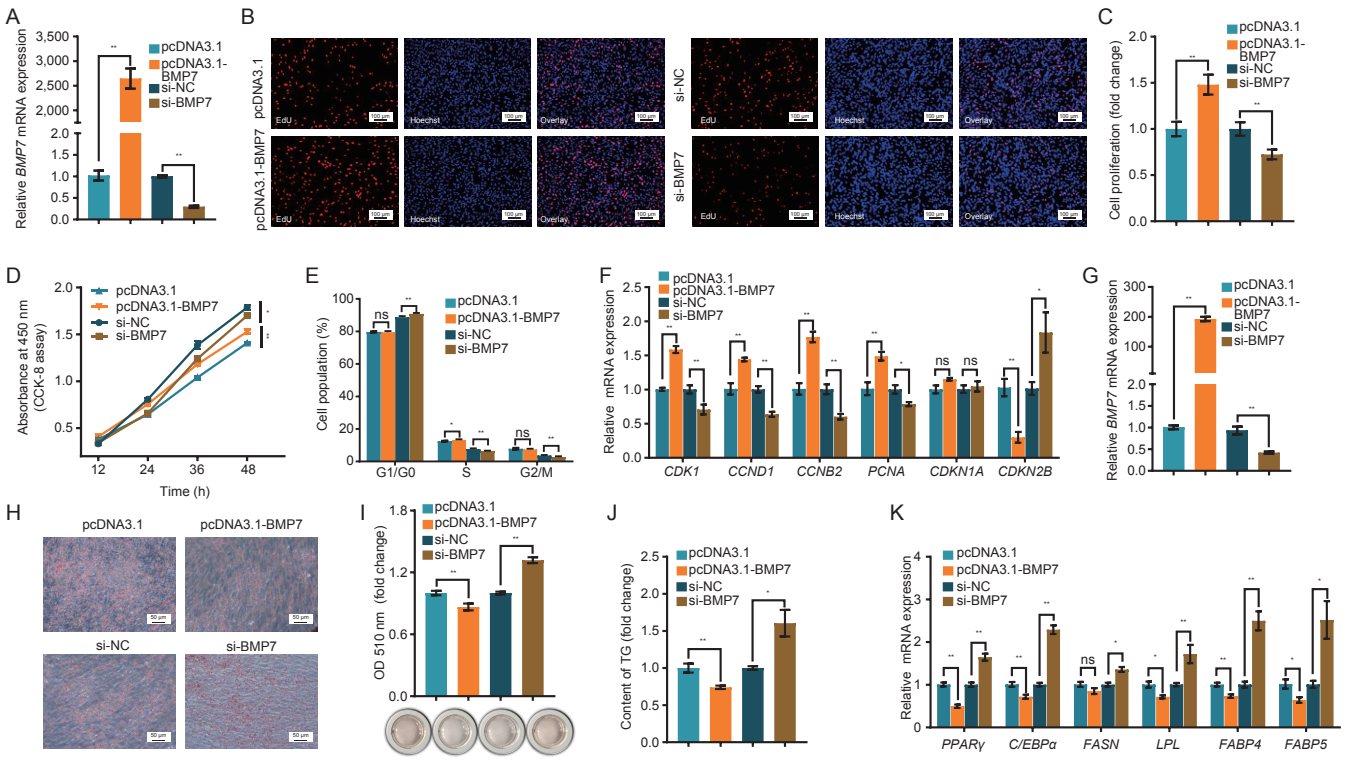


Fig. 8 *BMP7* promotes intramuscular fat primary preadipocytes (IMF-pre) proliferation and inhibits adipogenic differentiation. A, *BMP7* relative expression in IMF-pre was assessed 24 h after transfection with the listed nucleic acids. B, EdU proliferation assay after IMF-pre transfection. C, cell proliferation rate (flod change) of EdU-positive cell according to the statistical results. D, cell viability was determined using the CCK-8 assay. E, experimental and statistical results of cell cycle analysis using flow cytometry. F, relative expressions of *CDK1*, *CCND1*, *CCNB2*, *PCNA*, *CDKN1A*, and *CDKN2B*. G, *BMP7* relative expression in IMF-pre 48 h after transfection with the listed nucleic acids and induction of adipogenic differentiation. H, Oil Red O staining of adipogenically differentiated chicken myoblasts. I, spectrophotometric analysis of the lipid droplet content by Oil Red O staining of adipogenically differentiated chicken myoblasts. J, quantification of the intracellular TG content. K, the relative expressions of *PPARγ*, *C/EBPα*, *FASN*, *LPL*, *FABP4*, and *FABP5*. Data are mean±SE (n≥4). *, P<0.05; **, P<0.01; ns, not significant.

small interfering RNAs (si-NC and si-BMP7) into AbF-pre to evaluate their effects on proliferation and adipogenic differentiation. Compared to corresponding control group, the *BMP7* mRNA expression level exhibited an approximately 906-fold increase in myoblasts transfected with *BMP7* gene overexpression vector, and an approximately 79.18% decrease in myoblasts transfected with *BMP7* gene siRNA oligonucleotides (Fig. 9-A). EdU assays demonstrated that *BMP7* overexpression significantly increased the proliferation of AbF-pre, whereas the opposite effect was observed upon *BMP7* knockdown (P<0.05; Fig. 9-B and C). *BMP7* overexpression also significantly increased cell viability, whereas *BMP7* knockdown exhibited the opposite effect (P<0.01; Fig. 9-D). Moreover, the upregulation of *BMP7* expression resulted in a decrease in the proportion of cells in the G0/G1 phase and a significant increase in the proportion of cells in the S phase (P<0.05). Conversely, *BMP7* knockdown resulted in notable cell cycle arrest in the G1/G0 phase and a significant reduction in the proportion of cells in the S phase (P<0.01; Fig. 9-E; Appendix K). Additionally, *BMP7* overexpression resulted in significantly upregulated expression of *CDK1* and *CCND1* and downregulated expression of *CDKN1A* and *CDKN2B*, whereas *BMP7* knockdown had the opposite effect (P<0.05; Fig. 9-F). After adipogenic differentiation for 48 h, *BMP7* overexpression significantly promoted intracellular lipid droplets and TG content in AbF-pre, whereas *BMP7* knockdown reduced cellular lipid deposition (P<0.01; Fig. 9-G–J). The lipogenesis-related genes, including *FASN*, *C/EBPα*, *PPARγ*, *LPL*, *FABP4*, and *FABP5*, were significantly activated upon *BMP7* stimulation, whereas *BMP7* knockdown exhibited opposite effects (P<0.05; Fig. 9-K). Taken together, these data demonstrated that *BMP7* promotes AbF-pre proliferation and lipid synthesis.

4. Discussion

The BMPs are critical factors involved in bone and cartilage formation (Yan *et al.* 2017). However, their roles in growth, reproduction, and lipid deposition, particularly in chickens, remain unclear. In the present study, we successfully identified 14 members of the BMP family in the chicken. Phylogenetic analysis revealed that *BMP* genes could be classified into 5 subfamilies in chicken and other vertebrates, which was consistent with a study in fish (Ma *et al.* 2022). In addition, studies have demonstrated conserved motifs and domains in the *BMP* genes of both humans and fish (Mostofa

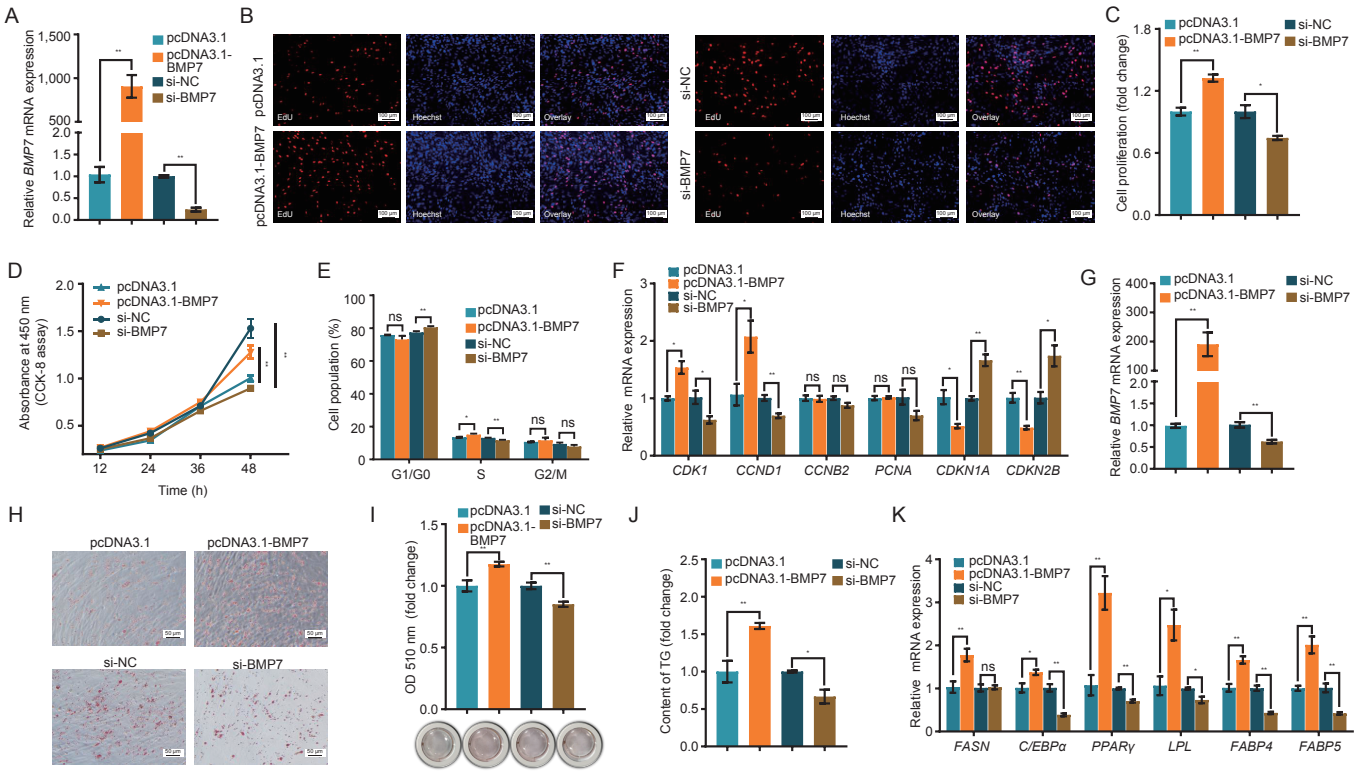


Fig. 9 BMP7 promotes abdominal fat primary preadipocytes (AbF-pre) proliferation and adipogenic differentiation. A, *BMP7* relative expression in intramuscular fat primary preadipocytes (IMF-pre) was assessed 24 h after transfection with the listed nucleic acids. B, EdU proliferation assay after AbF-pre transfection. C, cell proliferation rate (flod change) of EdU-positive cell according to the statistical results. D, cell viability was determined using the CCK-8 assay. E, experimental and statistical results of cell cycle analysis using flow cytometry. F, relative expressions of *CDK1*, *CCND1*, *CCNB2*, *PCNA*, *CDKN1A*, and *CDKN2B*. G, *BMP7* relative expression in AbF-pre 48 h after transfection with the listed nucleic acids and induction of adipogenic differentiation. H, Oil Red O staining of adipogenically differentiated chicken myoblasts. I, spectrophotometric analysis of the lipid droplet content by Oil Red O staining of adipogenically differentiated chicken myoblasts. J, quantification of the intracellular TG content. K, The relative expressions of *FASN*, *C/EBPα*, *PPARγ*, *LPL*, *FABP4*, and *FABP5*. Data are mean±SE (n≥3). *, P<0.05; **, P<0.01; ns, not significant.

et al. 2022), which were also observed in the present study. Moreover, researches have revealed variations in gene structures, amino acid sequences, and protein structures among *BMP* genes, suggesting potential differences in their biological functions (Lei *et al.* 2023).

Through natural and artificial directional selection, local and specialized commercial chickens exhibited significant phenotypic diversity, including variations in behavioral, morphological, and physiological traits (Rubin *et al.* 2010). Genetic variation served as a determinant of gene expression, thereby significantly contributed to the diversity observed in functional and phenotypic aspects (Beck *et al.* 2023). The PCA based on the SNPs of *BMP* genes revealed that genetic variations in *BMP* genes played a significant role in the breeding of laying hens and broilers. The breeding of commercial layer, broiler, and local chicken populations appears to be a collective response to the BMP family, as the analysis of SNP data for the individual genes revealed varying degrees of reduction or alteration in differentiation levels among different chicken breeds. Furthermore, correlation analysis established a significant association between genetic variations in the promoter region, exons, and introns of the genes and key traits, such as egg laying, growth, and serum lipid levels, thereby providing further support for the contribution of genetic variations in *BMP* genes to the formation of specific phenotypes.

The RNA-seq technology has been widely employed in the fields of epigenetics, biochemistry, and developmental differences, offering a means to evaluate the impact of genes on specific cellular or tissue physiological functions (Calabrese *et al.* 2013). Multi-tissue RNA-seq databases analyses revealed the differential expression of *BMP* genes in the abdominal fat, liver, cartilage, ovarian, and pectoral muscle tissues, and similar findings have been observed in humans (Robert *et al.* 2018; Wang L *et al.* 2019) and mice as well (Cameron *et al.* 2009; Friedrichs *et al.* 2011). Over the past a few years, extensive researches have demonstrated that specific molecules or genes could elicit markedly different biological effects in different tissues and cells (Chung *et al.* 2016; Wu *et al.* 2019; Huang *et al.* 2022). Our results indicated that *BMP7* was widely expressed in different tissues and organs, which was consistent with a previous report in mice (Danesh *et al.* 2009). BMP7 is a versatile growth factor that plays crucial roles in embryonic, skeletal, and neural development, reproductive regulation, and disease pathogenesis (Shimasaki *et al.* 2004; Katagiri and Watabe 2016; Aluganti Narasimhulu *et al.* 2020; Jensen *et al.* 2021). Despite the wealth of researches in humans and mice, there

was a notable scarcity of studies exploring the role of *BMP7* in chicken lipid metabolism and cellular functions.

In the present study, SNPs within *BMP7* intron region were significantly associated with body weight, breast muscle weight, leg weight, abdominal fat weight, and serum lipid levels. *BMP7* was differentially expressed in the liver, fat, and muscle RNA-seq databases, indicating that it may be involved in multicell proliferation and differentiation, as well as tissue lipid deposition. We found that *BMP7* was dynamically expressed during the proliferation and differentiation of myoblasts, IMF-pre, and AbF-pre, further clarifying the above-mentioned biological functions, as gene expression patterns were closely related to their functions (Zhang *et al.* 2022). Some studies have demonstrated that BMP7 promoted the proliferation of mouse skeletal muscle satellite cells and the formation of myotubes (Friedrichs *et al.* 2011), differentiation of pig intramuscular adipocytes (Zhou *et al.* 2010), and lipid accumulation in mature human beige adipocytes (Liu *et al.* 2022) and mouse liver (Boon *et al.* 2013). Other studies have reported that BMP7 reduced hepatic lipid accumulation in diet-induced obese mice (Boon *et al.* 2013), lipid deposition in adipocytes (Casana *et al.* 2022), and fat accumulation in muscle tissues (Narasimhulu and Singla 2023). Here, our data indicated that *BMP7* promoted the proliferation of myoblasts, IMF-pre, and AbF-pre, enhanced hepatocyte lipid synthesis, facilitated myoblasts differentiation, promoted myoblasts lipid deposition, and stimulated adipogenic differentiation of AbF-pre, while inhibited adipogenic differentiation of IMF-pre. Indeed, regulatory mechanisms of lipid synthesis and metabolism in IMF differed significantly from those in the liver, AbF, and muscle tissues in chicken (Nematbakhsh *et al.* 2021; Zhang M *et al.* 2021; Wang *et al.* 2023). A study reported that gene regulatory networks involved in cell development were different in IMF cells and AbF cells, in which AbF showed a higher capacity of lipid deposition than that in IMF in chicken (Zhang *et al.* 2019). Additionally, skeletal muscle cells and adipocytes could express specific genes or secrete specific factors to regulate lipid deposition (Komolka *et al.* 2014). Recent studies have showed that *BMP* genes could regulate lipid metabolism processes in the liver and adipose tissue through various genes or signaling pathways (Wang *et al.* 2013; An *et al.* 2021), which partially explained the variability of gene function within different cell types. Surprisingly, the *BMP7* gene showed higher expression level in the pectoral muscles of 1-wk-old LS chickens compared to that in AA broilers, and no differences in other stages, implying that the effects of *BMP* gene family on directed selection were achieved by synergetic interactions of the gene family members in chicken. A recent study also demonstrated that muscle development in native Chinese breeds and commercial broiler chickens was accompanied by the differential expression of related genes during different growth periods, and that muscle development was the result of the synergistic expression of multiple genes (Gu *et al.* 2022). However, the regulatory mechanisms of *BMP* family in myogenesis and adipogenesis require further investigation.

5. Conclusion

Collectively, our findings suggest that the *BMP* gene family is highly conserved during evolution and plays a crucial role in commercial chicken breeding. SNPs in *BMP* genes are significantly associated with growth performance, laying performance, and fat deposition. *BMP7* is dynamically expressed during myogenesis and adipogenesis, promotes the proliferation, differentiation, and lipid synthesis in myoblasts, enhances lipid synthesis in LMH cells, induces the proliferation and adipogenic differentiation of IMF-pre, stimulates the proliferation of AbF-pre, and inhibits the adipogenic differentiation of AbF-pre cells. These results provide new insights into the potential effects of the *BMP* gene family on the genetic and biological functions of poultry growth, egg production, and lipid metabolism.

Acknowledgements

This study was supported by the National Natural Science Foundation of China (32272867, 32372871 and 32172720) and the National Key Research and Development Program of China (2022YFF1000202).

Declaration of competing interest

The authors declare that they have no conflict of interest.

Declaration of generative AI and AI-assisted technologies in the writing process

The authors declare that they did not use AI in the preparation and writing of this manuscript.

Ethical approval

All animal experiments were approved by the Institutional Animal Care and Use Committee of the Henan Agricultural University (approval number: 11–0085). All birds were sacrificed by cervical dislocation according to the Laboratory Animal Guidelines for Euthanasia of the Chinese Association for Laboratory Animal Sciences (T/CALAS 31–2017).

Appendices associated with this paper are available at https://doi.org/10.1016/j.jia.2024.06.007

References

Aluganti Narasimhulu C, Singla D K. 2020. The role of bone morphogenetic protein 7 (BMP-7) in inflammation in heart diseases. *Cells*, **9**, 280.

An L, Shi Q, Zhu Y, Wang H, Peng Q, Wu J, Cheng Y, Zhang W, Yi Y, Bao Z. 2021. Bone morphogenetic protein 4 (BMP4) promotes hepatic glycogen accumulation and reduces glucose level in hepatocytes through mTORC2 signaling pathway. *Genes & Diseases*, **8**, 531–544.

Asharani P, Keupp K, Semler O, Wang W, Li Y, Thiele H, Yigit G, Pohl E, Becker J, Frommolt P. 2012. Attenuated BMP1 function compromises osteogenesis, leading to bone fragility in humans and zebrafish. *The American Journal of Human Genetics*, **90**, 661–674.

Bai D, Chen Y, Hu Y, He W F, Shi Y, Fan Q, Luo R, Li A. 2020. Transcriptome analysis of genes related to gonad differentiation and development in Muscovy ducks. *BMC Genomics*, **21**, 1–17.

Beck T, Rowlands T, Shorter T, Brookes A J. 2023. GWAS central: An expanding resource for finding and visualising genotype and phenotype data from genome-wide association studies. *Nucleic Acids Research*, **51**, D986–D993.

Boon M R, van den Berg S A, Wang Y, van den Bossche J, Karkampouna S, Bauwens M, De Saint-Hubert M, van der Horst G, Vukicevic S, de Winther M P. 2013. BMP7 activates brown adipose tissue and reduces diet-induced obesity only at subthermoneutrality. *PLoS ONE*, **8**, e74083.

Borok M J, Mademtzoglou D, Relaix F. 2020. Bu-MP-ing iron: How BMP signaling regulates muscle growth and regeneration. *Journal of Developmental Biology*, **8**, 4.

Bubner B, Baldwin I T. 2004. Use of real-time PCR for determining copy number and zygosity in transgenic plants. *Plant Cell Reports*, **23**, 263–271.

Calabrese C, Mangiulli M, Manzari C, Paluscio A M, Caratozzolo M F, Marzano F, Kurelac I, D'Erchia A M, D'Elia D, Licciulli F. 2013. A platform independent RNA-seq protocol for the detection of transcriptome complexity. *BMC Genomics*, **14**, 1–11.

Cameron T L, Belluoccio D, Farlie P G, Brachvogel B, Bateman J F. 2009. Global comparative transcriptome analysis of cartilage formation *in vivo*. *BMC Developmental Biology*, **9**, 1–17.

Carré G A, Couty I, Hennequet-Antier C, Govoroun M S. 2011. Gene expression profiling reveals new potential players of gonad differentiation in the chicken embryo. *PLoS ONE*, **6**, e23959.

Casana E, Jimenez V, Jambrina C, Sacristan V, Muñoz S, Rodo J, Grass I, Garcia M, Mallol C, León X. 2022. AAV-mediated BMP7 gene therapy counteracts insulin resistance and obesity. *Molecular Therapy-Methods & Clinical Development*, **25**, 190–204.

de Castro F C, Cruz M H C, Leal C L V. 2016. Role of growth differentiation factor 9 and bone morphogenetic protein 15 in ovarian function and their importance in mammalian female fertility-a review. *Asian–Australasian Journal of Animal Sciences*, **29**, 1065.

Chung K, Smith S, Choi S, Johnson B. 2016. Oleic acid enhances G protein coupled receptor 43 expression in bovine intramuscular adipocytes but not in subcutaneous adipocytes. *Journal of Animal Science*, **94**, 1875–1883.

Danesh S M, Villasenor A, Chong D, Soukup C, Cleaver O. 2009. BMP and BMP receptor expression during murine organogenesis. *Gene Expression Patterns*, **9**, 255–265.

Ducy P, Karsenty G. 2000. The family of bone morphogenetic proteins. *Kidney International*, **57**, 2207–2214.

Egerman M A, Cadena S M, Gilbert J A, Meyer A, Nelson H N, Swalley S E, Mallozzi C, Jacobi C, Jennings L L, Clay I. 2015. GDF11 increases with age and inhibits skeletal muscle regeneration. *Cell Metabolism*, **22**, 164–174.

Friedrichs M, Wirsdöerfer F, Flohé S B, Schneider S, Wuelling M, Vortkamp A. 2011. BMP signaling balances proliferation and differentiation of muscle satellite cell descendants. *BMC Cell Biology*, **12**, 1–17.

Gamer L W, Cox K A, Small C, Rosen V. 2001. *Gdf11* is a negative regulator of chondrogenesis and myogenesis in the developing chick limb. *Developmental Biology*, **229**, 407–420.

Goldman D C, Donley N, Christian J L. 2009. Genetic interaction between *Bmp2* and *Bmp4* reveals shared functions during multiple aspects of mouse organogenesis. *Mechanisms of Development*, **126**, 117–127.

Gu S, Wen C, Li J, Liu H, Huang Q, Zheng J, Sun C, Yang N. 2022. Temporal expression of myogenic regulatory genes in different chicken breeds during embryonic development. *International Journal of Molecular Sciences*, **23**, 10115.

Guo Y, Tang H, Li Z, Zhang Y, Li D, Li W, Sun G, Kang X, Han R. 2020. High-throughput transcriptome analysis reveals potentially important relationships between lncRNAs and genes in broilers affected by Valgus-varus deformity (*Gallus gallus*). *Gene*, **743**, 144511.

Guo Y, Zhang K, Geng W, Chen B, Wang D, Wang Z, Tian W, Li H, Zhang Y, Jiang R. 2023. Evolutionary analysis and functional characterization reveal the role of the insulin-like growth factor system in a diversified selection of chickens (*Gallus gallus*). *Poultry Science*, **102**, 102411.

Hopkins D R, Keles S, Greenspan D S. 2007. The bone morphogenetic protein 1/Tolloid-like metalloproteinases. *Matrix Biology*, **26**, 508–523.

Hou X, Tang Z, Liu H, Wang N, Ju H, Li K. 2012. Discovery of MicroRNAs associated with myogenesis by deep sequencing of serial developmental skeletal muscles in pigs. *PLoS ONE*, **7**, e52123.

Huang J, Guo D, Zhu R, Feng Y, Li R, Yang X, Shi D. 2022. FATP1 exerts variable effects on adipogenic differentiation and proliferation in cells derived from muscle and adipose tissue. *Frontiers in Veterinary Science*, **9**, 904879.

Jeanplong F, Falconer S J, Thomas M, Matthews K G, Oldham J M, Watson T, McMahon C D. 2012. Growth and differentiation factor-11 is developmentally regulated in skeletal muscle and inhibits myoblast differentiation. *Open Journal of Molecular and Integrative Physiology*, **2**,127–138.

Jensen G S, Leon-Palmer N E, Townsend K L. 2021. Bone morphogenetic proteins (BMPs) in the central regulation of energy balance and adult neural plasticity. *Metabolism*, **123**, 154837.

Ji H, Wang H, Ji Q, Ji W, Luo X, Wang J, Chai Z, Xin J, Cai X, Wu Z. 2020. Differential expression profile of microRNA in yak skeletal muscle and adipose tissue during development. *Genes & Genomics*, **42**, 1347–1359.

Jin M, Fei X, Li T, Lu Z, Chu M, Di R, He X, Wang X, Wei C. 2022. Transcriptome study digs out BMP2 involved in adipogenesis in sheep tails. *BMC Genomics*, **23**, 1–10.

Katagiri T, Watabe T. 2016. Bone morphogenetic proteins. *Cold Spring Harbor Perspectives in Biology*, **8**, a021899.

Kessler E, Takahara K, Biniaminov L, Brusel M, Greenspan D S. 1996. Bone morphogenetic protein-1: The type I procollagen C-proteinase. *Science*, **271**, 360–362.

Khorsand B, Elangovan S, Hong L, Dewerth A, Kormann M S, Salem A K. 2017. A comparative study of the bone regenerative effect of chemically modified RNA encoding BMP-2 or BMP-9. *The AAPS Journal*, **19**, 438–446.

Komolka K, Albrecht E, Wimmers K, Michal J J, Maak S. 2014. Molecular heterogeneities of adipose depots-potential effects on adipose-muscle cross-talk in humans, mice and farm animals. *Journal of Genomics*, **2**, 31.

Lei L, Zhu J, Chen C, Wang Y, Wu C, Qi M, Wang Y, Liu X, Hong X, Yu L. 2023. Genome-wide identification, evolution and expression analysis of bone morphogenetic protein (BMP) gene family in Chinese soft-shell turtle (*Pelodiscus sinensis*). *Frontiers in Genetics*, **14**, 1109478.

Li F, Liu J, Liu W, Gao J, Lei Q, Han H, Yang J, Li H, Cao D, Zhou Y. 2021. Genome-wide association study of body size traits in Wenshang Barred chickens based on the specific-locus amplified fragment sequencing technology. *Animal Science Journal*, **92**, e13506.

Li H, Wang T, Xu C, Wang D, Ren J, Li Y, Tian Y, Wang Y, Jiao Y, Kang X. 2015. Transcriptome profile of liver at different physiological stages reveals potential mode for lipid metabolism in laying hens. *BMC Genomics*, **16**, 763.

Li Z, Cai B, Abdalla B A, Zhu X, Zheng M, Han P, Nie Q, Zhang X. 2019. *LncIRS1* controls muscle atrophy *via* sponging miR15 family to activate IGF1-PI3K/AKT pathway. *Journal of Cachexia, Sarcopenia and Muscle*, **10**, 391–410.

Liu W, Li D, Yang M, Wang L, Xu Y, Chen N, Zhang Z, Shi J, Li W, Zhao S. 2022. GREM2 is associated with human central obesity and inhibits visceral preadipocyte browning. *EBioMedicine*, **78**, 103969.

Ma Y, Xiao Y, Xiao Z, Wu Y, Zhao H, Gao G, Wu L, Wang T, Zhao N, Li J. 2022. Genome-wide identification, characterization and expression analysis of the BMP family associated with beak-like teeth in Oplegnathus. *Frontiers in Genetics*, **13**, 938473.

McPherron A C, Lawler A M, Lee S J. 1999. Regulation of anterior/posterior patterning of the axial skeleton by growth/differentiation factor 11. *Nature Genetics*, **22**, 260–264.

Miyazono K, Kamiya Y, Morikawa M. 2010. Bone morphogenetic protein receptors and signal transduction. *Journal of Biochemistry*, **147**, 35–51.

Mostofa F, Yasid N A, Shamsi S, Ahmad S A, Mohd-Yusoff N F, Abas F, Ahmad S. 2022. In silico study and effects of BDMC33 on TNBS-induced *BMP* gene expressions in zebrafish gut inflammation-associated arthritis. *Molecules*, **27**, 8304.

Narasimhulu C A, Singla D K. 2023. BMP-7 attenuates sarcopenia and adverse muscle remodeling in diabetic mice *via* alleviation of lipids, inflammation, HMGB1, and pyroptosis. *Antioxidants*, **12**, 331.

Nematbakhsh S, Pei Pei C, Selamat J, Nordin N, Idris L H, Abdull Razis A F. 2021. Molecular regulation of lipogenesis, adipogenesis and fat deposition in chicken. *Genes*, **12**, 414.

Qiu Y Y, Zhang H S, Tang Y, Liu F Y, Pang J Q, Zhang X Y, Xiong H, Liang Y S, Zhao H Y, Chen S J. 2021. Mitochondrial dysfunction

resulting from the down-regulation of bone morphogenetic protein 5 may cause microtia. *Annals of Translational Medicine*, **9**, 5.
Robert A W, Angulski A B B, Spangenberg L, Shigunov P, Pereira I T, Bettes P S L, Naya H, Correa A, Dallagiovanna B, Stimamiglio M A. 2018. Gene expression analysis of human adipose tissue-derived stem cells during the initial steps of *in vitro* osteogenesis. *Scientific Reports*, **8**, 4739.
Rubin C J, Zody M C, Eriksson J, Meadows J R, Sherwood E, Webster M T, Jiang L, Ingman M, Sharpe T, Ka S. 2010. Whole-genome resequencing reveals loci under selection during chicken domestication. *Nature*, **464**, 587–591.
Shah T A, Rogers M B. 2018. Unanswered questions regarding sex and BMP/TGF-β signaling. *Journal of Developmental Biology*, **6**, 14.
Shao G, Luo L, Jiang S, Deng C, Xiong Y, Li F. 2011. AC/T mutation in microRNA target sites in *BMP5* gene is potentially associated with fatness in pigs. *Meat Science*, **87**, 299–303.
Sharma A, Huard C, Vernochet C, Ziemek D, Knowlton K M, Tyminski E, Paradis T, Zhang Y, Jones J E, von Schack D. 2014. Brown fat determination and development from muscle precursor cells by novel action of bone morphogenetic protein 6. *PLoS ONE*, **9**, e92608.
Shimasaki S, Moore R K, Otsuka F, Erickson G F. 2004. The bone morphogenetic protein system in mammalian reproduction. *Endocrine Reviews*, **25**, 72–101.
Urist M R. 1965. Bone: Formation by autoinduction. *Science*, **150**, 893–899.
Wang D, Li X, Zhang P, Cao Y, Zhang K, Qin P, Guo Y, Li Z, Tian Y, Kang X. 2022. ELOVL gene family plays a virtual role in response to breeding selection and lipid deposition in different tissues in chicken (*Gallus gallus*). *BMC Genomics*, **23**, 1–13.
Wang D, Qin P, Zhang K, Wang Y, Guo Y, Cheng Z, Li Z, Tian Y, Kang X, Li H. 2023. Integrated LC/MS-based lipidomics and transcriptomics analyses revealed lipid composition heterogeneity between pectoralis intramuscular fat and abdominal fat and its regulatory mechanism in chicken. *Food Research International*, **172**, 113083.
Wang L, Li J, Liu E, Kinnebrew G, Zhang X, Stover D, Huo Y, Zeng Z, Jiang W, Cheng L. 2019. Identification of alternatively-activated pathways between primary breast cancer and liver metastatic cancer using microarray data. *Genes*, **10**, 753.
Wang M S, Huo Y X, Li Y, Otecko N O, Su L Y, Xu H B, Wu S F, Peng M S, Liu H Q, Zeng L. 2016. Comparative population genomics reveals genetic basis underlying body size of domestic chickens. *Journal of Molecular Cell Biology*, **8**, 542–552.
Wang R N, Green J, Wang Z, Deng Y, Qiao M, Peabody M, Zhang Q, Ye J, Yan Z, Denduluri S. 2014. Bone morphogenetic protein (BMP) signaling in development and human diseases. *Genes & Diseases*, **1**, 87–105.
Wang S, Zhou G, Shu G, Wang L, Zhu X, Gao P, Xi Q, Zhang Y, Yuan L, Jiang Q. 2013. Glucose utilization, lipid metabolism and BMP-Smad signaling pathway of porcine intramuscular preadipocytes compared with subcutaneous preadipocytes. *Cellular Physiology and Biochemistry*, **31**, 981–996.
Wang Y, Liu S, Yan Y, Li S, Tong H. 2019. SPARCL1 promotes C2C12 cell differentiation *via* BMP7-mediated BMP/TGF-β cell signaling pathway. *Cell Death & Disease*, **10**, 852.
Wang Z, Yue Y X, Liu Z M, Yang L Y, Li H, Li Z J, Li G X, Wang Y B, Tian Y D, Kang X T. 2019. Genome-wide analysis of the FABP gene family in liver of chicken (*Gallus gallus*): Identification, dynamic expression profile, and regulatory mechanism. *International Journal of Molecular Sciences*, **20**, 5948.
Wu F J, Luo C W. 2014. Characterization of the signaling and ovarian functions of bone morphogenetic protein 8. *Endocrine Abstracts*, **35**, P665.
Wu W, Zhang D, Yin Y, Ji M, Xu K, Huang X, Peng Y, Zhang J. 2019. Comprehensive transcriptomic view of the role of the *LGALS12* gene in porcine subcutaneous and intramuscular adipocytes. *BMC Genomics*, **20**, 1–13.
Yan L, Gao R, Liu Y, He B, Lv S, Hao D. 2017. The pathogenesis of ossification of the posterior longitudinal ligament. *Aging and Disease*, **8**, 570.
Yang Z, Li P, Shang Q, Wang Y, He J, Ge S, Jia R, Fan X. 2020. CRISPR-mediated BMP9 ablation promotes liver steatosis *via* the down-regulation of PPARα expression. *Science Advances*, **6**, eabc5022.
Ying Y, Liu X M, Marble A, Lawson K A, Zhao G Q. 2000. Requirement of *Bmp8b* for the generation of primordial germ cells in the mouse. *Molecular Endocrinology*, **14**, 1053–1063.
Zhang C, Xu X, Xu X, Li Y, Zhao P, Chen X, Shen X, Zhang Z, Chen Y, Liu S. 2022. Genome-wide identification, evolution analysis of cytochrome *P450* monooxygenase multigene family and their expression patterns during the early somatic embryogenesis in *Dimocarpus longan* Lour. *Gene*, **826**, 146453.
Zhang M, Li F, Ma X, Li W, Jiang R, Han R, Li G, Wang Y, Li Z, Tian Y. 2019. Identification of differentially expressed genes and pathways between intramuscular and abdominal fat-derived preadipocyte differentiation of chickens *in vitro*. *BMC Genomics*, **20**, 1–15.
Zhang M, Ma X, Zhai Y, Zhang D, Sui L, Li W, Jiang R, Han R, Li G, Li Z. 2020. Comprehensive transcriptome analysis of lncRNAs reveals the role of lncAD in chicken intramuscular and abdominal adipogenesis. *Journal of Agricultural and Food Chemistry*, **68**, 3678–3688.
Zhang M, Zheng D, Peng Z, Zhu Y, Li R, Wu Q, Li Y, Li H, Xu W, Zhang M. 2021. Identification of differentially expressed genes and lipid metabolism signaling pathways between muscle and fat tissues in broiler chickens. *The Journal of Poultry Science*, **58**, 131–137.
Zhang Y, Wang Y, Li Y, Wu J, Wang X, Bian C, Tian Y, Sun G, Han R, Liu X. 2021. Genome-wide association study reveals the genetic determinism of growth traits in a Gushi-Anka F_2 chicken population. *Heredity*, **126**, 293–307.
Zhang Z, Yang W, Cao Y, Shi Y, Lei C, Du B, Li X, Zhang Q. 2015. The functions of BMP3 in rabbit articular cartilage repair. *International Journal of Molecular Sciences*, **16**, 25934–25946.
Zhao G, Liaw L, Hogan B L. 1998. Bone morphogenetic protein 8A plays a role in the maintenance of spermatogenesis and the integrity of the epididymis. *Development*, **125**, 1103–1112.
Zhong S, Wang Y, Li J, Wang M, Meng L, Ma Z, Zhang S, Liu Z. 2018. Spatial and temporal expression of *bmp8a* and its role in regulation of lipid metabolism in zebrafish Danio rerio. *Gene Reports*, **10**, 33–41.
Zhou G, Wang S, Wang Z, Zhu X, Shu G, Liao W, Yu K, Gao P, Xi Q, Wang X. 2010. Global comparison of gene expression profiles between intramuscular and subcutaneous adipocytes of neonatal landrace pig using microarray. *Meat Science*, **86**, 440–450.
Zimmers T A, Jiang Y, Wang M, Liang T W, Rupert J E, Au E D, Marino F E, Couch M E, Koniaris L G. 2017. Exogenous GDF11 induces cardiac and skeletal muscle dysfunction and wasting. *Basic Research in Cardiology*, **112**, 1–12.

Executive Editor-in-Chief Kui Li
Managing Editor Han Zhang